[9] McNamara II JO, Andrechek ER, Wang Y, Viles KD, Rempel RE, Gilboa E, et al. Cell type-specific delivery of siRNAs with aptamer-siRNA chimeras. Nat Biotechnol 2006;24:1005–15.
[10] Li SD, Chen YC, Hackett MJ, Huang L. Tumor-targeted delivery of siRNA by self-assembled nanoparticles. Mol Ther 2008;16:163–9.
[11] Wang XL, Xu R, Wu X, Gillespie D, Jensen R, Lu ZR. Targeted systemic delivery of a therapeutic siRNA with a multifunctional carrier controls tumor proliferation in mice. Mol Pharm 2009;6:738–46.
[12] Davis ME, Zuckerman JE, Choi CHJ, Seligson D, Tolcher A, Alabi CA, et al. Evidence of RNAi in humans from systemically administered siRNA via targeted nanoparticles. Nature 2010;64:1067–70.
[13] Christie RJ, Matsumoto Y, Miyata K, Nomoto T, Fukushima S, Osada K, et al. Targeted polymeric micelles for siRNA treatment of experimental cancer by intravenous injection. ACS Nano 2012;6:5174–89.
[14] Dohmen C, Edinger D, Frohlich T, Schreiner L, Lachelt U, Troiber C, et al. Nanosized multifunctional polyplexes for receptor-mediated siRNA delivery. ACS Nano 2012;26:5198–208.
[15] Lee H, Lytton-Jean AKR, Chen Y, Love KT, Park AI, Karagiannis ED, et al. Molecularly self-assembled nucleic acid nanoparticles for targeted in vivo siRNA delivery. Nat Nanotechnol 2012;7:389–93.
[16] Kim HJ, Ishii T, Zheng M, Watanabe S, Toh K, Matsumoto Y, et al. Multifunctional polyion complex micelle featuring enhanced stability, targetability, and endosome escapability for systemic siRNA delivery to subcutaneous model of lung cancer. Drug Deliv Transl Res 2014;4:50–60.
[17] Jule E, Nagasaki Y, Kataoka K. Surface plasmon resonance study on the interaction between lactose-installed poly(ethylene glycol)-poly(D, L-lactide) block copolymer micelles and lectins immobilized on a gold surface. Langmuir 2002;18:10334–9.
[18] Alam MR, Ming X, Fisher M, Lackey JG, Rajeev KG, Manoharan M, et al. Multivalent cyclic RGD conjugates for targeted delivery of small interfering RNA. Bioconjug Chem 2011;22:1673–81.
[19] Harada A, Kataoka K. Formation of polyion complex micelles in an aqueous milieu from a pair of oppositely-charged block copolymers with poly(ethylene glycol) segments. Macromolecules 1995;28:5294–9.
[20] Kataoka K, Togawa H, Harada A, Yasugi K, Matsumoto T, Katayose S. Spontaneous formation of polyion complex micelles with narrow distribution from antisense oligonucleotide and cationic block copolymer in physiological saline. Macromolecules 1996;29:8556–7.
[21] Kakizawa Y, Kataoka K. Block copolymer micelles for delivery of gene and related compounds. Adv Drug Deliv Rev 2002;54:203–22.
[22] Miyata K, Nishiyama N, Kataoka K. Rational design of smart supramolecular assemblies for gene delivery: chemical challenges in the creation of artificial viruses. Chem Soc Rev 2012;41:2562–74.
[23] Kim HJ, Oba M, Pittella F, Nomoto T, Cabral H, Matsumoto Y, et al. PEG-detachable cationic polyaspartamide derivatives bearing stearoyl moieties for systemic siRNA delivery toward subcutaneous BxPC3 pancreatic tumor. J Drug Target 2012;20:33–42.
[24] Kakizawa Y, Harada A, Kataoka K. Environment-sensitive stabilization of core-shell structured polyion complex micelle by reversible cross-linking of the core through disulfide bond. J Am Chem Soc 1999;121:11247–8.
[25] Matsumoto S, Christie RJ, Nishiyama N, Miyata K, Ishii A, Oba M, et al. Environment-responsive block copolymer micelles with a disulfide cross-linked core for enhanced siRNA delivery. Biomacromolecules 2009;10:119–27.
[26] Christie RJ, Miyata K, Matsumoto Y, Nomoto T, Menasco D, Lai TC, et al. Effect of polymer structure on micelles formed between siRNA and cationic block copolymer comprising thiols and amidines. Biomacromolecules 2011;12:3174–85.
[27] Meister A, Anderson ME. Glutathione. Annu Rev Biochem 1983;52:711–60.
[28] Saito G, Swanson JA, Lee KD. Drug delivery strategy utilizing conjugation via reversible disulfide linkages: role and site of cellular reducing activities. Adv Drug Deliv Rev 2013;55:199–215.
[29] Soutschek J, Akinc A, Bramlage B, Charisse K, Constien R, Donoghue M, et al. Therapeutic silencing of an endogenous gene by systemic administration of modified siRNAs. Nature 2004;432:173–8.
[30] Oba M, Miyata K, Osada K, Christie RJ, Sanjoh M, Li W, et al. Polyplex micelles prepared from ω-cholesteryl PEG-polycation block copolymers for systemic gene delivery. Biomaterials 2011;32:652–63.
[31] Oba M, Fukushima S, Kanayama N, Aoyagi K, Nishiyama N, Koyama H, et al. Cyclic RGD peptide-conjugated polyplex micelles as a targetable gene delivery system directed to cells possessing αvβ3 and αvβ5 integrins. Bioconjug Chem 2007;18:1415–23.
[32] Matsumoto Y, Nomoto T, Cabral H, Mastumoto Y, Watanabe S, Christie RJ, et al. Direct and instantaneous observation of intravenously injected substances using intravital confocal micro-videography. Biomed Opt Express 2010;1:1209–16.
[33] Ruoslahti E. RGD and recognition sequences for integrins. Annu Rev Cell Dev Biol 1996;12:697–715.
[34] Xiong J, Stehle T, Zhang R, Joachimiak A, Frech M, Goodman S, et al. Crystal structure of the extra-cellular segment of integrin αvβ3 in complex with an Arg-Gly-Asp ligand. Science 2002;296:151–5.
[35] Itaka K, Yamauchi K, Harada A, Nakamura K, Kawaguchi H, Kataoka K. Polyion complex micelles from plasmid DNA and poly(ethyleneglycol)-poly(L-lysine) block copolymer as serum-tolerable polyplex system: physicochemical properties of micelles relevant to gene transfection efficiency. Biomaterials 2003;24:4495–506.
[36] Zukerman JE, Choi CHJ, Han H, Davis ME. Polycation-siRNA nanoparticles can disassemble at the kidney glomerular basement membrane. Proc Natl Acad Sci U S A 2012;109:3137–42.
[37] Shayakhmetov DM, Eberly AM, Li ZY, Lieber A. Deletion of penton RGD motifs affects the efficiency of both the internalization and the endosome escape of viral particles containing adenovirus serotype 5 or 35 fiber knobs. J Virol 2005;79:1053–61.
[38] Symonds P, Murray JC, Hunter AC, Debska G, Szewczyk A, Moghimi SM. Low and high molecular weight poly(L-lysine)s/poly(L-lysine)-DNA complexes initiate mitochondrial-mediated apoptosis differently. FEBS Lett 2005;579:6191–8.
[39] Wolfrum C, Shi S, Jayaprakash KN, Jayaraman M, Wang G, Pandey RK, et al. Mechanisms and optimization of *in vivo* delivery of lipophilic siRNAs. Nat Biotechnol 2007;25:1149–57.

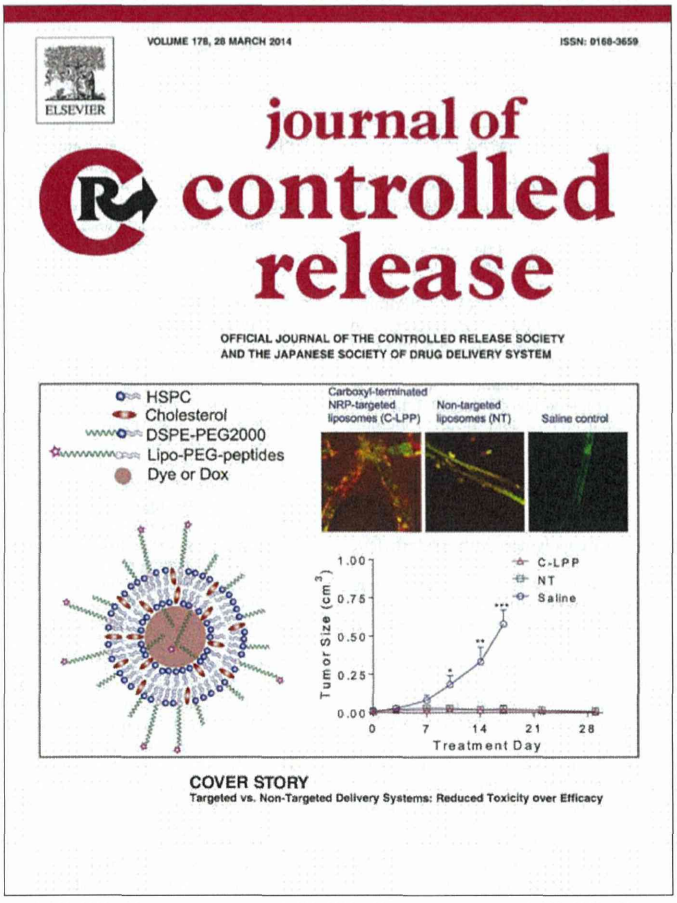

Journal of Controlled Release 178 (2014) 18–24

Contents lists available at ScienceDirect

Journal of Controlled Release

journal homepage: www.elsevier.com/locate/jconrel

Systemic siRNA delivery to a spontaneous pancreatic tumor model in transgenic mice by PEGylated calcium phosphate hybrid micelles

Frederico Pittella [a,b], Horacio Cabral [b], Yoshinori Maeda [b], Peng Mi [c], Sumiyo Watanabe [a], Hiroyasu Takemoto [c], Hyun Jin Kim [d], Nobuhiro Nishiyama [c], Kanjiro Miyata [a,*], Kazunori Kataoka [a,b,d,e,**]

[a] Center for Disease Biology and Integrative Medicine, Graduate School of Medicine, The University of Tokyo, 7-3-1 Hongo, Bunkyo-ku, Tokyo 113-0033, Japan
[b] Department of Bioengineering, Graduate School of Engineering, The University of Tokyo, 7-3-1 Hongo, Bunkyo-ku, Tokyo 113-8656, Japan
[c] Polymer Chemistry Division, Chemical Resources Laboratory, Tokyo Institute of Technology, R1-11, 4259 Nagatsuta, Midori-ku, Yokohama 226-8503, Japan
[d] Department of Materials Engineering, Graduate School of Engineering, The University of Tokyo, 7-3-1 Hongo, Bunkyo-ku, Tokyo 113-8656, Japan
[e] Center for NanoBio Integration, The University of Tokyo, 7-3-1 Hongo, Bunkyo-ku, Tokyo 113-8656, Japan

ARTICLE INFO

Article history:
Received 3 August 2013
Accepted 7 January 2014
Available online 15 January 2014

Keywords:
siRNA delivery
Calcium phosphate
PEG
Charge-conversional polymer
Transgenic mice
Spontaneous pancreatic carcinoma

ABSTRACT

Efficient systems for delivery of small interfering RNA (siRNA) are required for clinical application of RNA interference (RNAi) in cancer therapy. Herein, we developed a safe and efficient nanocarrier comprising poly(ethylene glycol)-*block*-charge-conversional polymer (PEG-CCP)/calcium phosphate (CaP) hybrid micelles for systemic delivery of siRNA and studied their efficacy in spontaneous bioluminescent pancreatic tumors from transgenic mice. PEG-CCP was engineered to provide the siRNA-loaded hybrid micelles with enhanced colloidal stability and biocompatibility due to the PEG capsule and with endosome-disrupting functionality due to the acidic pH-responsive CCP segment where the polyanionic structure could be converted to polycationic structure at acidic pH through *cis*-aconitic amide cleavage. The resulting hybrid micelles were confirmed to have a diameter of <50 nm, with a narrow size distribution. Intravenously injected hybrid micelles significantly reduced the luciferase-based luminescent signal from the spontaneous pancreatic tumors in an siRNA sequence-specific manner. The gene silencing activity of the hybrid micelles correlated with their preferential tumor accumulation, as indicated by fluorescence imaging and histological analysis. Moreover, there were no significant changes in hematological parameters in mice treated with the hybrid micelles. These results demonstrate the great potential of the hybrid micelles as siRNA carriers for RNAi-based cancer therapy.

1. Introduction

Small interfering ribonucleic acid (siRNA) provides new perspectives for the treatment of various diseases. It functions by obstructing a specific cellular process by reducing protein production in a sequence-specific manner, a phenomenon termed RNA interference (RNAi) [1–4]. In particular, the use of RNAi-based therapy is expected to have potential for treatment of cancer because cancerous cells overexpress several specific genes, including oncogenes [5,6]. In the development of an RNAi-based cancer therapy, systemic administration of siRNA is essential for its effective accumulation in the wide range of internal tumor tissues. However, intravenous injection of naked siRNA molecules results in their rapid enzymatic degradation and subsequent clearance through the kidneys [7,8]. Therefore, efficient carriers are required to ensure successful delivery of siRNA to the therapeutic site of action [3,6,9].

Calcium phosphate (CaP)-based nanocarriers, a promising delivery system, has been widely developed for delivering nucleic acids to mammalian cells [10–14]. These are readily prepared by mixing aqueous ionic solutions for efficient encapsulation of nucleic acids. In this regard, we have previously prepared poly(ethylene glycol) (PEG)-coated CaP hybrid micelles by utilizing PEG-polyanion block copolymers [12,15–20]. In these block copolymers, the polyanion segment acts as a binding moiety with CaP nanoparticles, whereas the PEG segment forms a nonionic and hydrophilic outer layer for enhanced colloidal stability and biocompatibility (Fig. 1A). Furthermore, our recent studies successfully demonstrated functionalization of the polyanion segment for efficient endosomal escape of the siRNA payload [19–21]. An acidic pH-responsive anionic moiety, *cis*-aconitic amide (Aco), was introduced into the cationic side chain of the endosome-disrupting polyaspartamide derivative, poly{*N*′-[*N*-(2-aminoethyl)-2-aminoethyl] aspartamide} (PAsp(DET)) (Fig. 1B). The obtained PAsp(DET-Aco) bearing a net negative charge was found to be inactive for membrane disruption at extracellular neutral pH. However, on reversion to the parent polycation PAsp(DET) by cleavage of the Aco moiety at endosomal acidic pH, membrane disruptivity was activated [thus, termed charge-conversional polymer (CCP)] (Fig. 1C) [22]. Ultimately, the systemic administration of PEG-CCP/CaP hybrid micelles carrying

* Corresponding author. Tel.: +81 3 5841 1701; fax: +81 3 5841 7139.
** Correspondence to: K. Kataoka, Center for Disease Biology and Integrative Medicine, Graduate School of Medicine, The University of Tokyo, 7-3-1 Hongo, Bunkyo-ku, Tokyo 113-0033, Japan. Tel.: +81 3 5841 7138; fax: +81 3 5841 7139.
E-mail addresses: miyata@bmw.t.u-tokyo.ac.jp (K. Miyata), kataoka@bmw.t.u-tokyo.ac.jp (K. Kataoka).

0168-3659/$ – see front matter © 2014 Elsevier B.V. All rights reserved.
http://dx.doi.org/10.1016/j.jconrel.2014.01.008

vascular endothelial growth factor (VEGF) siRNA achieved significant antitumor activity in a murine xenograft model of subcutaneous pancreatic tumors [20]. These results demonstrated the great potential of this system for use as a cancer therapy and motivated us to investigate this system further.

To confirm the translational capability of promising nanocarriers, relevant preclinical tumor models, which parallel the microenvironment characteristics of tumors in the clinic, should be considered. In animal tumor models prepared by implantation of exogenous cancer cells or tissues, the tumoral microenvironment presents substantial differences with that of tumors in patients, including stroma, vasculature, lymphatics, immune cells, and increased population of certain clonal fractions due to selective stresses during cell culture or tissue transplantation [23,24]. These features in transplanted models are expected to affect the nanocarrier-mediated delivery of siRNA as well as drugs, *e.g.*, efficiencies of penetration, accumulation, and gene silencing in tumor tissues. In this regard, in genetically engineered tumor models, the tumor development closely relates to the clinical setting of the disease, with immune responses, angiogenesis, and inflammation naturally interrelating with the tumor [23]. Therefore, by using such spontaneous tumor models, siRNA-loaded nanocarriers could be evaluated in tumors with more relevant microenvironment and cell populations.

In the present study, we applied siRNA-loaded hybrid micelles in a genetically engineered pancreatic tumor model, in which the tumor gradually arises *in situ* and is associated with normal immune, angiogenesis, and inflammatory processes. The EL1-Luc/TAg transgenic mice used in this study spontaneously develop bioluminescent pancreatic adenocarcinoma owing to the SV40 T and firefly luciferase transgene constructs, which are regulated by the rat EL1 promoter [25]. SV40 T alters molecular, physiological, and histological aspects comparable to the tumorigenesis of acinar cell carcinoma in humans. Moreover, EL1-Luc/TAg transgenic mice permit non-invasive tracing of tumors through bioluminescence imaging because the cancer cells exclusively express luciferase. Accordingly, *in vivo* RNAi activity of the hybrid micelles carrying luciferase siRNA (siLuc) was determined by quantifying the luminescent signal from the pancreatic tumors after intravenous injection. To verify the validity of the measured RNAi activity, the tumor accumulation profile of the hybrid micelles was further assessed. To the best of our knowledge, this is the first study to demonstrate the effective delivery of siRNA to a spontaneous tumor model in transgenic mice by systemic administration.

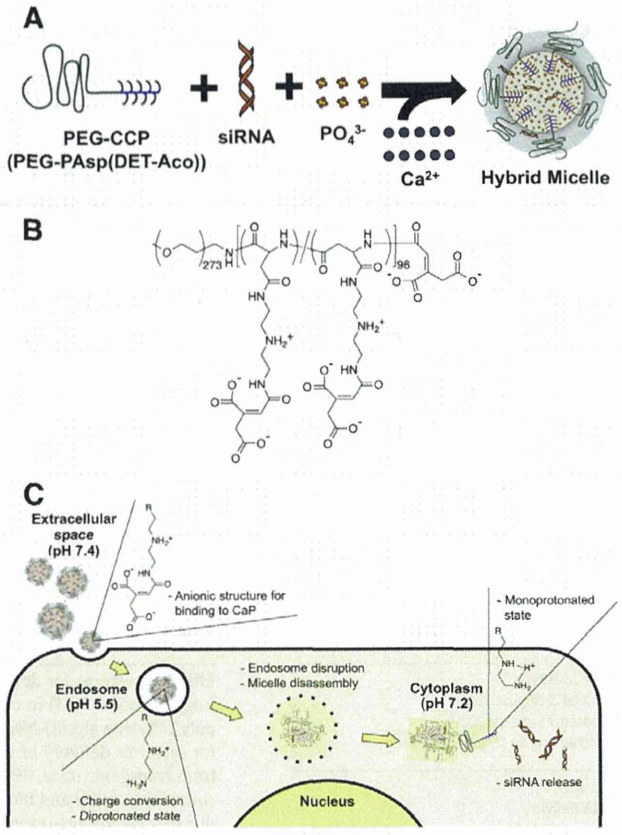

Fig. 1. (A) Schematic illustration of the preparation of hybrid micelles with PEG-CCP, siRNA, and CaP. (B) Chemical structure of PEG-PAsp(DET-Aco), termed PEG-CCP. (C) Schematic illustration of the cellular delivery of siRNA by PEG-CCP/CaP hybrid micelles. At extracellular neutral pH, PEG-CCP binds to the CaP nanoparticle, generating a PEG outer layer. Once endocytosed by the cell, the hybrid micelles undergo endosomal acidification. During acidification, PEG-CCP is converted to the parent PEG-PAsp(DET) through cleavage of the *cis*-aconitic amide bond, exposing the diprotonated side chain structure for endosomal membrane disruption. Finally, the siRNA payload is released into the cytoplasm, while the PAsp(DET) segment adopts the membrane-inactive monoprotonated side chain at cytoplasmic neutral pH.

2. Materials and methods

2.1. Materials, cell lines, and animals

$CaCl_2$ (anhydrous), Na_3PO_4, NaCl, HCl, ethanol, and phosphate buffered saline (PBS) were purchased from Wako Pure Chemical Industries Ltd. (Osaka, Japan). Dulbecco's modified Eagle's medium (DMEM) and penicillin/streptomycin stabilized solution were purchased from Sigma-Aldrich (St. Louis, MO). *In vivo* grade luciferin VivoGlo, cell culture lysis buffer, and the Luciferase Assay System were purchased from Promega Corporation (Madison, WI). Tissue-Tek OCT compound and fetal bovine serum (FBS) were acquired from Sakura Finetek USA, Inc. (Torrance, CA) and Dainippon Sumitomo Pharma Co., Ltd. (Osaka, Japan), respectively. Methoxy-poly(ethylene glycol)-*block*-poly(*N*″-{*N*′-[(*N*-*cis*-aconityl)-2-aminoethyl]-2-aminoethyl}aspartamide) (PEG-PAsp(DET-Aco) or PEG-CCP) was synthesized as previously described, and then characterized by ^{1}H NMR (PEG: 12 kDa; PAsp(DET-Aco): 34 kDa) [19,20]. Firefly luciferase siRNA (siLuc) and its control siRNA (siScr) were synthesized by Hokkaido System Science (Hokkaido, Japan). The sequences of the siLuc were: 5′-CUU ACG CUG AGU ACU UCG AdTdT-3′ (sense) and 5′-UCG AAG UAC UCA GCG UAA GdTdT-3′ (antisense); the sequences of the siScr were: 5′-UUC UCC GAA CGU GUC ACG UdTdT-3′ (sense) and 5′-ACG UGA CAC GUU CGG AGA AdTdT-3′ (antisense). Fluorescently labeled siLuc was obtained by introducing Alexa Fluor 647 to the 5′ end of sense strand from GeneDesign, Inc. (Osaka, Japan).

HeLa-Luc, a firefly luciferase-expressing human cervical cancer cell line, was purchased from Caliper Life Science (Hopkinton, MA). The cells were maintained in DMEM containing 10% FBS and 1% streptomycin/penicillin in a humidified atmosphere containing 5% CO_2 at 37 °C. FVB/NJc1 female mice (18–20 g, 6 weeks) were purchased from Clea Japan, Inc. (Tokyo, Japan). EL1-Luc/EL1-SV40 T-antigen transgenic mice (OncoMouse; male, 18–20 g, 6 weeks) were purchased from Caliper Life Sciences (Hopkinton, MA). Female FVB mice and male transgenic mice were allowed to breed, and the newborn mice were genotyped primarily by basal bioluminescence imaging at the age of 5 weeks. Male mice presenting basal luminescence in the pancreas were separated for use in the experiments. All animal experiments were performed in accordance with the Guidelines for the Care and Use of Laboratory Animals as stated by The University of Tokyo.

2.2. Preparation of hybrid micelles

Hybrid micelles were prepared as previously described [20]. In brief, a solution of 2.5 M $CaCl_2$ (1 μL) was diluted in 10 mM Tris buffer (pH 10) (11.5 μL). Another solution containing PEG-CCP (1.0 mg/mL) in 10 mM Tris/HCl buffer (pH 7.5) was mixed with a solution of 15 μM siRNA in 10 mM HEPES buffer (pH 7.2) and with 50 mM HEPES buffer containing 1.5

mM Na_3PO_4 and 140 mM NaCl (pH 7.5) (2.5 μL:5 μL:5 μL). The former solution was mixed with the latter solution by pipetting up and down for approximately 20 s (final siRNA concentration: 3 μM). The freshly prepared micelle solution containing 40 μg siRNA and 100 μg PEG-CCP (1 mL) was then purified and concentrated using a VivaSpin-06 device (molecular weight cut-off (MWCO): 10 kDa). The ultrafiltration was performed in a swing bucket rotor at 900 *g* and 4 °C for 20 min. To minimize non-specific binding of micelles to the membrane, the centrifuge filter devices were washed with de-ionized water before use. After centrifugation, the retained solution (100 μL) was added to 300 mM NaCl solution (100 μL) to adjust the final concentration to 150 mM NaCl. Through this procedure, the excess free calcium ions were removed from the micelle solution to the flow-through. The quantity of calcium removed was determined using a calcium sensitive dye, arsenazo III, by the SRL Laboratories (SRL Inc., Tokyo, Japan).

2.3. Transmission electron microscopic (TEM) imaging

Hybrid micelle solution (20 μL) was loaded on a 400-mesh copper grid and stained with 20 μL of uranyl acetate solution (2%, w/v) for 5 s. The copper grids with carbon-coated collodion film were glow-discharged for 10 s with an Eiko IB-3 ion coater (Eiko Engineering Co. Ltd., Japan) prior to use. The morphology of hybrid micelles was observed on a JEM-1400 (JEOL Ltd., Tokyo, Japan) with 100 kV acceleration voltage and 40 μA beam current, toward high resolution and high contrast with high performance imaging of specimens.

2.4. In vitro luciferase gene silencing

HeLa-Luc cells were seeded in a 96-well plate at a cell density of 2500 cells/well in 0.1 mL of DMEM containing 10% FBS and then precultured for 24 h. Before transfection, the medium was refreshed. Hybrid micelles containing siRNA (siLuc or siScr), hybrid micelles without siRNA (mock), or naked siRNA (siLuc or siScr) were applied to each well to final siRNA concentrations of 100 and 200 nM (n = 6). After 48 h of incubation, the medium was removed and the cells were washed twice with 100 μL of PBS. The cells were then lysed with 50 μL of cell culture lysis buffer. The luciferase expression in the lysate was determined from photoluminescence intensity using the Luciferase Assay System and Mithras LB 940 (Berthold Technologies). The relative luciferase activity was calculated as a ratio to that in non-treated cells.

2.5. Biodistribution and tumor accumulation of hybrid micelles in transgenic mice

Mice were fed with alfalfa-free food *ad libitum*. A group of three male transgenic mice (15 weeks) were intravenously injected with Alexa Fluor 647-labeled siLuc (Alexa647-siLuc) contained in hybrid micelles (200 μL, 20 μg siRNA). As a control, the same amount of naked Alexa647-siLuc was also injected to another group of male transgenic mice. Intravenous injection was performed slowly (10 s per injection) to avoid adverse side effects. Mice were sacrificed 6 h after the injection, and then the main organs (heart, lungs, liver, spleen, kidneys, and pancreas, including tumors) were excised for fluorescent imaging using IVIS (Caliper Life Sciences, Hopkinton, MA). Organs were washed in PBS and kept on ice prior to analysis. Similarly, blood was collected from mice at 6 h after the injection, and then it was centrifuged at 2000 *g* for 10 min to obtain the plasma. The fluorescence intensity was determined using the Living Image software through the selection of an ROI around the whole organ/tumor and the plasma, and then it was converted to the % of dose/g of tissue (or plasma) based on a standard curve. To avoid incomplete separation of tumors from the pancreas, the combined weight of the organ and tumors was used for the subsequent statistical data analysis.

2.6. Tumor histology

After the biodistribution studies described in the preceding section were complete, a portion of the pancreas/tumor tissue from each mouse was rapidly frozen in Tissue-Tek OCT compound with liquid nitrogen in ethanol. The frozen pancreas/tumor tissues embedded in the block were then cut into 6-μm thick slices at −20 °C with a Tissue-Tek Cryo3 microtome/cryostat (Sakura Finetek USA, Inc., Torrance, CA). Each section of the pancreas/tumor tissue was fixed with formalin and stained with hematoxylin and eosin (HE) for histological identification of tumor cells and healthy pancreatic cells. In addition to HE staining, adjacent cryosections of the pancreas/tumor tissue were stained with Hoechst 33342 (Dojindo Lab., Kumamoto, Japan) for observation of cellular nuclei using a confocal laser scanning microscope (CLSM) (LSM 510, Carl Zeiss, Germany). The CLSM observation was performed at the excitation wavelengths of 633 nm (He–Ne laser) and 710 nm (MaiTai laser, two photon excitation) for Alexa647-siRNA and Hoechst 33342, respectively. The fluorescence intensities of the Alexa647-siRNA from the tumor region or the healthy pancreatic region in the obtained CLSM image were determined using the ImageJ software.

2.7. In vivo luminescence reduction in transgenic mice

Hybrid micelle solutions containing 20 μg of siLuc or siScr (200 μL) were slowly injected into the caudal vein of transgenic mice (13 weeks; n = 16). Bioluminescence intensity in the pancreatic tumors was determined before injection and 24 h after injection of the hybrid micelles using an IVIS instrument. Mice were anesthetized with isoflurane and luciferin was injected intraperitoneally at a dosage of 150 mg/kg (200 μL). Measurements were performed 10 min after luciferin injection for three different positions in each mouse (right flank, left flank, and ventral positions) to reduce variability in bioluminescence due to the tumor positions. Photons emitted from the pancreas region were quantified using the Living Image software and summed from the 3 positions. All images were set to the same conditions and color scale.

2.8. Hematological parameters and cytokine levels

Hybrid micelle solutions containing 20 μg of siScr (200 μL) were slowly injected in the caudal vein of female Balb/c mice (6 weeks). Blood was collected at several time points after the injection and centrifuged at 2000 *g* for 10 min to obtain the plasma. The levels of alkaline phosphatase (ALP), aspartate aminotransferase (AST), alanine aminotransferase (ALT), and creatinine (Cr) in the plasma were measured by the SRL Laboratories (SRL Inc., Tokyo, Japan) (n = 5). Also, the levels of tumor necrosis factor-α (TNF-α), interleukin-6 (IL-6), IL-1α, and IL-1β in plasma were determined by Quantikine® ELISA kits, according to the manufacturer's protocol (n = 4).

3. Results and discussion

3.1. Preparation of hybrid micelles

Preparation of CaP nanoparticles in an aqueous solution is known to result in the formation of insoluble large aggregates over time. Thus, PEG-CCP (Fig. 1B) was used to prepare CaP nanoparticles with enhanced colloidal stability through the steric repulsive effect of the PEG capsule. These nanoparticles also had endosome-disrupting functionality derived from the CCP segment. This segment was synthesized through the introduction of an Aco moiety into the side chain of PAsp(DET) through *cis*-aconitic amide bond formation. Successful preparation of PEG-CCP (or quantitative introduction of the Aco moiety) was confirmed using ^{1}H NMR spectroscopy (data not shown), as previously described [19]. The resulting PAsp(DET-Aco) segment was stable at neutral pH, whereas under acidic conditions, it underwent *cis*-aconitic amide cleavage to revert back to the parent PAsp(DET) (Fig. 1C) [22].

The generated PAsp(DET) enabled acidic pH-selective membrane disruption based on the distinctive change in the protonation state of the side chain unit, *i.e.*, the monoprotonated state at neutral pH and the diprotonated state at acidic pH, directed toward endosomal escape of the payload (Fig. 1C) [26,27].

The hybrid micelles were prepared by simple mixing of a solution containing PEG-CCP, siRNA, and phosphate ions, with a solution of calcium ions (Fig. 1A). The prepared micelles were then subjected to ultrafiltration (MWCO: 10 kDa) for the removal of excess free calcium ions as well as for concentration of the sample. The concentrated solution was diluted with the same volume of NaCl solution (300 mM) to generate the hybrid micelle solution at 150 mM NaCl. The obtained hybrid micelles were observed with a high performance TEM. Fig. 2A depicts spherical nanoparticles of approximately 30 nm in diameter with a clearly narrow size distribution, which was confirmed by the size distribution histogram obtained from analyses of the TEM images (mean diameter: 33.2 nm, n = 111) (Fig. 2B). The hybrid micelle solution was further characterized by dynamic light scattering (DLS) and electrophoretic light scattering. The size of hybrid micelles was 38 nm at the peak of the number-weighted histogram in DLS (Supporting Fig. S1), associated with a narrow size distribution (polydispersity index = 0.09). This size is consistent with that estimated from the TEM images. Further, the zeta-potential of hybrid micelles was almost neutral (−2.2 mV), consistent with the presence of nonionic PEG outer layer. In addition, the DLS analysis revealed that the cumulant size of the hybrid micelles was maintained over 7 days of storage at 4 °C (data not shown), demonstrating the potential for long-term storage in a refrigerator.

3.2. In vitro luciferase gene silencing

To confirm *in vitro* siRNA delivery efficacy, the hybrid micelles carrying siLuc were applied to a luciferase assay with cultured HeLa-Luc cells as a luciferase-expressing model cell line. After 48 h of incubation, siLuc delivered by the hybrid micelles significantly decreased the luciferase expression in a dose-dependent manner (Fig. 3); the hybrid micelles inhibited approximately 50% and 90% of luciferase expression at 100 nM and 200 nM siRNA, respectively. In sharp contrast, the hybrid micelles with a control sequence of siRNA (siScr) as well as the mock micelles without siRNA resulted in no reduction in luciferase expression, indicating sequence-specific, potent gene silencing ability of the hybrid micelles. In our previous studies, the hybrid micelles exhibited a significant gene silencing effect on endogenous VEGF in cultured pancreatic cancer cells (PanC-1 and BxPC3) [19,20], suggesting that their gene silencing ability is not limited to a specific target gene and cell line. The efficient gene silencing ability of the hybrid micelles was probably due to the stable encapsulation of siRNA in CaP nanoparticles in cell culture medium [20], followed by efficient cellular internalization and endosomal escape induced by the CCP segment [19]. With regard to the cellular internalization, our previous study revealed that hybrid micelles were efficiently uptaken by HeLa cells within 4 h, probably due to an energy-dependent endocytosis [16]. It should be noted that no significant cytotoxicity was observed for any of the samples at the tested concentrations, as determined in a cell viability assay using a water soluble tetrazolium salt (WST-8) (data not shown).

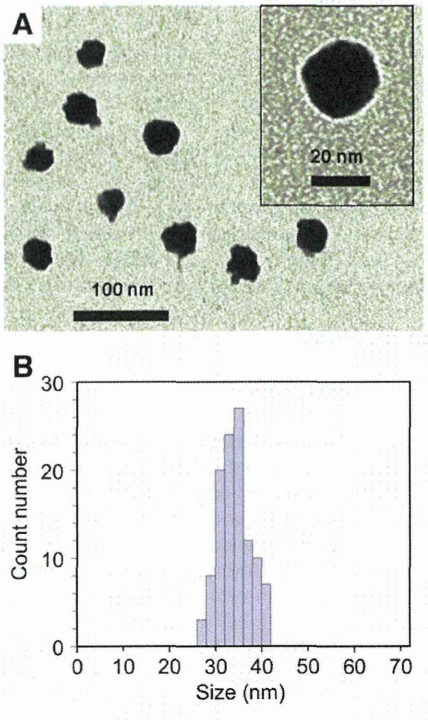

Fig. 2. (A) TEM image of the hybrid micelles. (B) Size distribution histogram of the hybrid micelles based on their TEM images.

3.3. Biodistribution and tumor accumulation of hybrid micelles in transgenic mice

Biodistribution of hybrid micelles after intravenous injection was evaluated in the transgenic mice presenting spontaneous pancreatic tumors using Alexa647-siRNA. At 6 h after injection, the transgenic mice were sacrificed, and the organs were excised for measuring fluorescence intensity, which was then converted to the % of dose/g of tissue based on a standard curve. As the border between a pancreatic tumor and healthy pancreas tissue is unclear, the fluorescence intensity of the whole pancreatic tissue was measured for tumor accumulation of Alexa647-siRNA. Note that the significant fluorescence was not detected from the collected blood samples, indicating that almost all the hybrid micelles (or Alexa647-siRNAs) were eliminated from the bloodstream within 6 h. Thus, the fluorescence intensity measured from each organ would not be affected by blood circulating micelles. As shown in Fig. 4, the amount of hybrid micelles was approximately 0.9% of dose/g of pancreas/tumor, which was 6-fold larger than that in naked siRNA. No significant difference between hybrid micelles and naked siRNA was observed for the accumulation in other organs; however, the kidneys displayed lower accumulation for Alexa647-siRNA delivered by the hybrid micelles compared to naked siRNA. These results suggest that the hybrid micelles could protect Alexa647-siRNA from rapid renal filtration, enabling it to circulate for longer in the blood, and therefore accumulate more in the pancreas/tumor.

The enhanced accumulation of hybrid micelles in the pancreas/tumor was further investigated by histological analysis. First, HE-stained sections were prepared to facilitate distinction of the tumor region (T) from healthy pancreatic tissue (H). As depicted in Fig. 5A, healthy pancreatic cells were organized into lobules toward formation of glandular acini. In contrast, tumor cells show a non-organized solid growth pattern [28,29]. Fig. 5A also shows the presence of connective tissue septa in between the T and H areas. CLSM was then performed to image the corresponding Hoechst 33342-stained sections. It is noteworthy that fluorescence signals from Alexa647-siRNA delivered by hybrid micelles were found mainly in the tumor region (Fig. 5B). Quantitative analysis using the ImageJ software indicated that the fluorescence signal of Alexa647-siRNA in the tumor region was 2.9-fold stronger than that in the healthy pancreas. By considering that the average weight of pancreas/tumor in the transgenic mice was 2.2-fold higher than that of pancreas in wild-type mice, the tumor accumulation of siRNA delivered by hybrid micelles can be roughly estimated to be ~1.3% of dose/g of tumor with the assumption that the tissue weights are similar between tumor and healthy pancreas in the transgenic mice. Thus, the

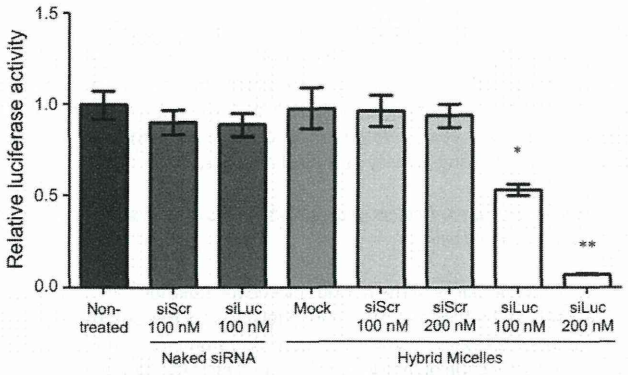

Fig. 3. *In vitro* luciferase gene silencing by hybrid micelles in cultured HeLa-Luc cells. Luciferase luminescence was quantified after 48 h of incubation of cells treated with samples. Results are expressed as mean and standard deviation (n = 6). $^{*}P < 0.05$; $^{**}P < 0.001$ (ANOVA followed by Newman–Keuls).

preferential tumor accumulation of siRNA-loaded hybrid micelles was demonstrated in the spontaneous pancreatic tumor model.

In a previous study, we reported that the tumor vasculature in the EL1-Luc/TAg transgenic mice was covered with pericytes [30], which can considerably limit the penetration of nanocarriers into the spontaneous tumor model in comparison to hypervascular and/or less stromal tumor models [31,32]. Nevertheless, the hybrid micelles apparently penetrated and distributed within the tumors (Fig. 5B). This behavior should be attributed to the relatively small size of the hybrid micelles (approximately 30–40 nm in diameter, Fig. 2 and Supporting Fig. S1), facilitating the passage of the nanocarriers through the tumor vasculature and stromal tissues. This was in agreement with our recent study where <50-nm polymeric micelles efficiently penetrated into the tissue, even in hypopermeable tumor models, which was in contrast to the control micelles that were >50 nm in size [33]. It should be further noted that the enhanced tumor accumulation behavior of hybrid micelles, compared to naked siRNA, in the present spontaneous pancreatic tumors was comparable to our previous observation in a subcutaneous BxPC3 tumor model [20]. This can also be explained by the small size of hybrid micelles, as the small-sized nanocarriers may be less affected by the tumor microenvironments restricting extravasation and penetration of nanocarriers, such as pericyte coverage of the vasculature [33]. Altogether, the hybrid micelles are a promising strategy for the systemic delivery of siRNA to various and whole tumor tissues/cells.

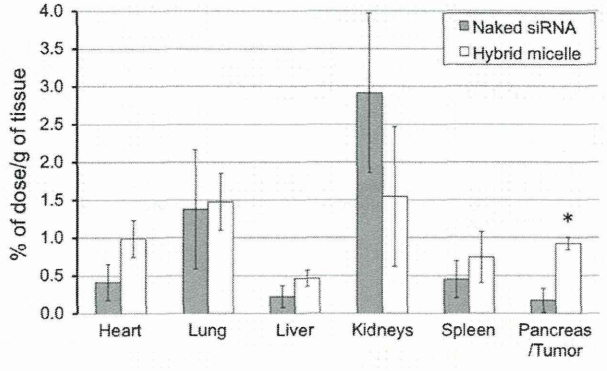

Fig. 4. Biodistribution of Alexa647-siRNA-loaded hybrid micelles and naked Alexa647-siRNA by fluorescence quantification at 6 h after intravenous injection (20 μg siRNA/injection) in 14-week-old transgenic mice. The obtained fluorescence intensities were converted to % of dose/g of tissue based on a standard curve. Results are expressed as mean and standard error of mean (n = 3). ANOVA followed by Newman–Keuls ($^{*}P < 0.01$).

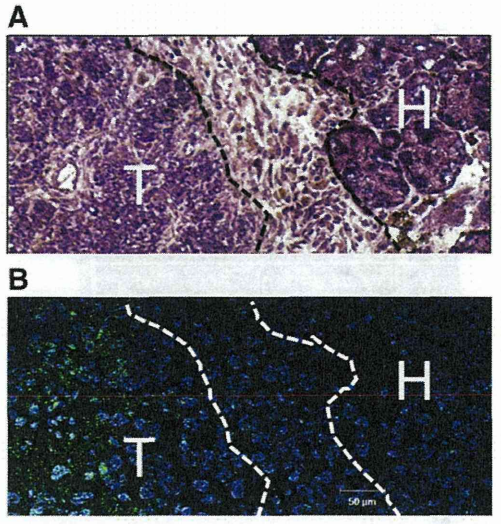

Fig. 5. Histological observation of pancreas/tumor in transgenic mice treated with hybrid micelles. Sections were prepared from the pancreas/tumor tissue excised at 6 h after intravenous injection of hybrid micelles carrying Alexa647-siRNA (20 μg siRNA/injection) to transgenic mice. (A) HE staining: non-organized tumor cells (T) and healthy pancreatic structure in lobes (H) are separated by the dotted line. (B) CLSM image of an adjacent section to that stained with HE. Nuclei (blue) were stained with Hoechst 33342, and Alexa647-siRNA is shown in green.

3.4. In vivo luciferase gene silencing in transgenic mice

Pancreatic cancer is considered to be one of the most fatal cancers [34]. Moreover, the all-stage 5-year survival has not improved greatly during the last 25 years [35]. These facts have motivated us to develop novel therapeutics to improve the prognosis of pancreatic cancer patients. An immunocompetent mouse presenting spontaneous pancreatic tumors is a useful model for establishment of such novel therapeutics, including anticancer drug-loaded micelles [30]. Herein, the *in vivo* gene silencing activity of hybrid micelles was evaluated with the spontaneous pancreatic tumor model developed in EL1-Luc/TAg transgenic mice, in which the expression of firefly luciferase is promoted specifically in the acinar cell carcinoma [25]. Accordingly, this model can be used for a gene silencing assay that employs the bioluminescence of the pancreatic tumors. It is worth noting that the following characteristics were confirmed for the spontaneous pancreatic cancer model in the previous study [30]; i) liver and intestine metastases are likely to occur in this model after the mice becoming 16 weeks old, ii) the pancreas/tumor in this model is enlarged and also the pancreatic cancer may grow over the normal position of pancreas, and iii) the bioluminescent signal from the pancreatic cancer is not always emitted from the same anatomic position. Considering these points, the bioluminescence measurements in this study were performed for 3 different positions, i.e., left flank, frontal, and right flank of the 13-week-old mice without detectable tumor metastases.

Representative bioluminescence images of the left flank position of mice treated with or without siLuc-loaded hybrid micelles are shown in Fig. 6A, where the variable bioluminescence signals from the pancreatic tumor can be identified. At 24 h after systemic injection of the hybrid micelles, the bioluminescence intensity in the pancreatic tumors exhibited a significant reduction of 61% compared with the initial intensity before injection (Fig. 6B; $P < 0.01$), indicating that the hybrid micelles induced efficient luciferase gene silencing in the tumor tissue. There was no significant reduction in the bioluminescence signal after injection of siScr-loaded hybrid micelles, indicating that the reduction in the bioluminescence intensity was due to the sequence-specific

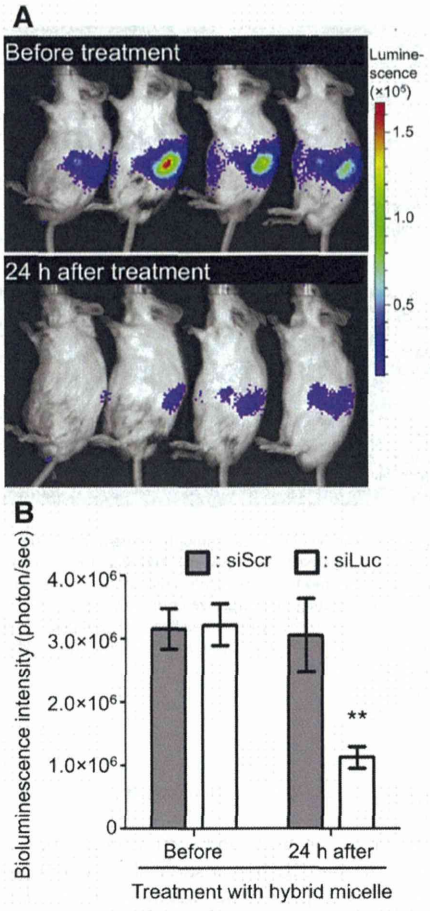

Fig. 6. *In vivo* gene silencing activity of systemically administered hybrid micelles in the spontaneous pancreatic tumors of transgenic mice. (A) Representative images of mice before and 24 h after injection of hybrid micelles containing siLuc (20 μg siRNA/mouse). (B) Bioluminescence intensity in the pancreatic tumors after intravenous injection of hybrid micelles containing siLuc or siScr (20 μg siRNA/mouse). Results are expressed as mean and standard deviation (n = 16). ANOVA followed by Newman–Keuls (**$P < 0.01$).

RNAi machinery. The similar gene silencing profile of hybrid micelles was further observed for the protein amount of luciferase in homogenized pancreas/tumor tissues (Supporting Fig. S2). This sequence-specific gene silencing activity of hybrid micelles is consistent with their significantly enhanced tumor accumulation of the siRNA payload (Figs. 4 and 5), which was roughly estimated to be ~1.3% of dose/g of tumor, corresponding to ~40 ng siRNA. Interestingly, the *in vivo* gene silencing efficacy of hybrid micelles in the spontaneous pancreatic cancer cells (60% with ~40 ng siRNA) was apparently higher than the *in vitro* efficacy in the cultured HeLa-Luc cells (50% with ~130 ng siRNA). These different efficacies might be due to varying cellular innate functions between the *in vivo* pancreatic cancer cells and the *in vitro* monolayer-cultured cervical cancer cells. The cellular innate functions, including the expression levels of luciferase and RNAi-related genes, are known to be substantially altered between live tissue and cell culture, especially monolayer culture, and also different types of cells [36–38]. Indeed, the luciferase expression in the present pancreatic cancer cells was lost in monolayer culture. This is the reason for the use of HeLa-Luc cells as a conventional cancer cell line for demonstrating the *in vitro* gene silencing activity of hybrid micelles.

3.5. Hematological parameters and cytokine levels after systemic administration of hybrid micelles

To verify the safety of the hybrid micelle formulation, hematological parameters and inflammatory cytokine levels were measured at several time points after systemic administration. As summarized in Table 1, the intravenous injection of hybrid micelles induced no remarkable changes in the levels of AST, ALT, and ALP as indicators of liver function and that of Cr as an indicator of kidney function over 48 h, suggesting negligible adverse side effects on the liver and the kidneys. Similarly, the levels of inflammatory cytokines, *i.e.*, TNF-α, IL-6, IL-1α, and IL-1β, were not affected by the injection of hybrid micelles (Supporting Fig. S3). Overall, it was demonstrated that the intravenous injection of hybrid micelles induced no severe acute toxicity under the tested conditions.

4. Conclusion

In the present study, hybrid micelles prepared with a smart block copolymer PEG-CCP were applied for systemic siRNA delivery to spontaneous pancreatic tumors in EL1-Luc/TAg transgenic mice. The obtained results confirmed the enhanced accumulation of siRNA-loaded hybrid micelles in the tumor tissue and their significant gene silencing activity. Notably, this was associated with negligible changes in hematological parameters. Altogether, the great potential of the hybrid micelles for RNAi-based cancer therapy was successfully demonstrated.

Acknowledgment

This research was funded by the Japan Society for the Promotion of Science (JSPS) through the "Funding Program for World-Leading Innovative R&D on Science and Technology (FIRST Program)," the Adaptable and Seamless Technology Transfer Program through Target-driven R&D (A-STEP), the National Institute of Biomedical Innovation (NIBIO), and Grants-in-Aid for Scientific Research from the Japanese Ministry of Health, Labour and Welfare. Part of this work was conducted in the Research Hub for Advanced Nano Characterization, The University of Tokyo, supported by the Ministry of Education, Culture, Sports, Science and Technology (MEXT), Japan. The authors are grateful to S. Ogura and K. Date for their assistance with animal care.

Appendix A. Supplementary data

Supplementary data to this article can be found online at http://dx.doi.org/10.1016/j.jconrel.2014.01.008.

References

[1] A. Fire, S. Xu, M.K. Montgomery, S.A. Kostas, S.E. Driver, C.C. Mello, Potent and specific genetic interference by double-stranded RNA in *Caenorhabditis elegans*, Nature 391 (1998) 806–811.

Table 1
Hematological parameters after intravenous injection of hybrid micelles (20 μg siRNA/mouse).

	Non-treated (0 min)	10 min	30 min	60 min	120 min	20 h	48 h
AST (U/L)	40 ± 5	38 ± 9	42 ± 4	40 ± 5	41 ± 5	36 ± 4	47 ± 7
ALT (U/L)	61 ± 18	62 ± 13	73 ± 5	67 ± 8	64 ± 12	86 ± 28	61 ± 23
ALP (U/L)	401 ± 25	401 ± 22	424 ± 10	378 ± 8	384 ± 23	377 ± 28	477 ± 37
Cr (mg/dL)	0.11 ± 0.01	0.11 ± 0.01	0.11 ± 0.01	0.10 ± 0.01	0.10 ± 0.01	0.10 ± 0.02	0.07 ± 0.01

Abbreviations: AST, aspartate aminotransferase; ALT, alanine aminotransferase; ALP, alkaline phosphatase; Cr, creatinine. Results are expressed as mean and standard deviation (n = 5).

[2] S.M. Elbashir, J. Harborth, W. Lendeckel, A. Yalcin, K. Weber, T. Tuschl, Duplexes of 21-nucleotide RNAs mediate RNA interference in cultured mammalian cells, Nature 411 (2001) 494–498.
[3] K. Whitehead, R. Langer, D. Anderson, Knocking down barriers: advances in siRNA delivery, Nat. Rev. Drug Discov. 8 (2009) 129–138.
[4] J.C. Burnett, J.J. Rossi, RNA-based therapeutics: current progress and future prospects, Chem. Biol. 19 (2012) 60–71.
[5] F. Takeshita, T. Ochiya, Therapeutic potential of RNA interference against cancer, Cancer Sci. 97 (2006) 689–696.
[6] Y.-K. Oh, T.G. Park, siRNA delivery systems for cancer treatment, Adv. Drug Deliv. Rev. 61 (2009) 850–862.
[7] F. van de Water, O. Boerman, A. Wouterse, J. Peters, F. Russel, R. Masereeuw, Intravenously administered short interfering RNA accumulates in the kidney and selectively suppresses gene function in renal proximal tubules, Drug Metab. Dispos. 34 (2006) 1393–1397.
[8] J. Turner, S. Jones, S. Moschos, M. Lindsay, M. Gait, MALDI-TOF mass spectral analysis of siRNA degradation in serum confirms an RNase A-like activity, Mol. Biosyst. 3 (2007) 43–50.
[9] R.J. Christie, N. Nishiyama, K. Kataoka, Delivering the code: polyplex carriers for deoxyribonucleic acid and ribonucleic acid interference therapies, Endocrinology 151 (2010) 466–473.
[10] C.A. Chen, H. Okayama, Calcium phosphate-mediated gene-transfer—a highly efficient transfection system for stably transforming cells with plasmid DNA, Biotechniques 6 (1988) 632.
[11] M. Jordan, A. Schallhorn, F.M. Wurm, Transfecting mammalian cells: optimization of critical parameters affecting calcium-phosphate precipitate formation, Nucleic Acids Res. 24 (1996) 596–601.
[12] Y. Kakizawa, K. Kataoka, Block copolymer self-assembly into monodispersive nanoparticles with hybrid core of antisense DNA and calcium phosphate, Langmuir 18 (2002) 4539–4543.
[13] M. Zhang, K. Kataoka, Nano-structured composites based on calcium phosphate for cellular delivery of therapeutic and diagnostic agents, Nano Today 4 (2009) 508–517.
[14] J. Li, Y.C. Chen, Y.C. Tseng, S. Mozumdar, L. Huang, Biodegradable calcium phosphate nanoparticle with lipid coating for systemic siRNA delivery, J. Control. Release 142 (2010) 416–421.
[15] Y. Kakizawa, K. Miyata, S. Furukawa, K. Kataoka, Size-controlled formation of a calcium phosphate-based organic–inorganic hybrid vector for gene delivery using poly(ethylene glycol)-block-poly(aspartic acid), Adv. Mater. 16 (2004) 699–702.
[16] Y. Kakizawa, S. Furukawa, K. Kataoka, Block copolymer-coated calcium phosphate nanoparticles sensing intracellular environment for oligodeoxynucleotide and siRNA delivery, J. Control. Release 97 (2004) 345–356.
[17] Y. Kakizawa, S. Furukawa, A. Ishii, K. Kataoka, Organic–inorganic hybrid-nanocarrier of siRNA constructing through the self-assembly of calcium phosphate and PEG-based block aniomer, J. Control. Release 111 (2006) 368–370.
[18] M. Zhang, A. Ishii, N. Nishiyama, S. Matsumoto, T. Ishii, Y. Yamasaki, K. Kataoka, PEGylated calcium phosphate nanocomposites as smart environment-sensitive carriers for siRNA delivery, Adv. Mater. 21 (2009) 3520–3525.
[19] F. Pittella, M. Zhang, Y. Lee, H.J. Kim, T. Tockary, K. Osada, T. Ishii, K. Miyata, N. Nishiyama, K. Kataoka, Enhanced endosomal escape of siRNA-incorporating hybrid nanoparticles from calcium phosphate and PEG-block charge-conversional polymer for efficient gene knockdown with negligible cytotoxicity, Biomaterials 32 (2011) 3106–3114.
[20] F. Pittella, K. Miyata, Y. Maeda, T. Suma, Q. Chen, R.J. Christie, K. Osada, N. Nishiyama, K. Kataoka, Pancreatic cancer therapy by systemic administration of VEGF siRNA contained in calcium phosphate/charge-conversional polymer hybrid nanoparticles, J. Control. Release 161 (2012) 868–874.
[21] H. Takemoto, K. Miyata, S. Hattori, T. Ishii, T. Suma, S. Uchida, N. Nishiyama, K. Kataoka, Acidic pH-responsive siRNA conjugate for reversible carrier stability and accelerated endosomal escape with reduced IFNα-associated immune response, Angew. Chem. Int. Ed. 52 (2013) 6218–6221.
[22] Y. Lee, K. Miyata, M. Oba, T. Ishii, S. Fukushima, M. Han, H. Koyama, N. Nishiyama, K. Kataoka, Charge conversion ternary polyplex with endosomes disruption moiety: a technique for efficient and safe gene delivery, Angew. Chem. Int. Ed. 120 (2008) 5241–5244.
[23] K.K. Frese, D.A. Tuveson, Maximizing mouse cancer models, Nat. Rev. Cancer 7 (2007) 654–658.
[24] G. Francia, W. Cruz-Munoz, S. Man, P. Xu, R.S. Kerbe, Mouse models of advanced spontaneous metastasis for experimental therapeutics, Nat. Rev. Cancer 11 (2011) 135–141.
[25] N. Zhang, S. Lyons, E. Lim, P. Lassota, A spontaneous acinar cell carcinoma model for monitoring progression of pancreatic lesions and response to treatment through noninvasive bioluminescence imaging, Clin. Cancer Res. 15 (2009) 4915–4924.
[26] K. Miyata, M. Oba, M. Nakanishi, S. Fukushima, Y. Yamasaki, H. Koyama, N. Nishiyama, K. Kataoka, Polyplexes from poly(aspartamide) bearing 1,2-diaminoethane side chains induce pH-selective, endosomal membrane destabilization with amplified transfection and negligible cytotoxicity, J. Am. Chem. Soc. 130 (2008) 16287–16294.
[27] K. Miyata, N. Nishiyama, K. Kataoka, Rational design of smart supramolecular assemblies for gene delivery: chemical challenges in the creation of artificial viruses, Chem. Soc. Rev. 41 (2012) 2562–2574.
[28] L.A. Aaltonen, S.R. Hamilton, World Health Organization; international agency for research on cancer, in: L.A. Aaltonen, S.R. Hamilton (Eds.), Pathology and Genetics of Tumours of the Digestive System, IARC Press: Oxford University Press, Lyon: Oxford, 2000, (314 pp.).
[29] R.A. Caruso, A. Inferrera, G. Tuccari, G. Barresi, Acinar cell carcinoma of the pancreas, a histologic, immunocytochemical and ultrastructural study, Histol. Histopathol. 9 (1994) 53–58.
[30] H. Cabral, M. Murakami, H. Hojo, Y. Terada, M.R. Kano, U.-I. Chung, N. Nishiyama, K. Kataoka, Targeted therapy of spontaneous murine pancreatic tumors by polymeric micelles prolongs survival and prevents peritoneal metastasis, Proc. Natl. Acad. Sci. U. S. A. 110 (2013) 11397–11402.
[31] M.R. Kano, Y. Bae, C. Iwata, Y. Morishita, M. Yashiro, M. Oka, T. Fujii, A. Komuro, K. Kiyono, M. Kaminishi, K. Hirakawa, Y. Ouchi, N. Nishiyama, K. Kataoka, K. Miyazono, Improvement of cancer-targeting therapy, using nanocarriers for intractable solid tumors by inhibition of TGF-β signaling, Proc. Natl. Acad. Sci. U. S. A. 104 (2007) 3460–3465.
[32] L. Zhang, H. Nishihara, M.R. Kano, Pericyte-coverage of human tumor vasculature and nanoparticle permeability, Biol. Pharm. Bull. 35 (2012) 761–766.
[33] H. Cabral, Y. Matsumoto, K. Mizuno, Q. Chen, M. Murakami, M. Kimura, Y. Terada, M.R. Kano, K. Miyazono, M. Uesaka, N. Nishiyama, K. Kataoka, Accumulation of sub-100 nm polymeric micelles in poorly permeable tumours depends on size, Nat. Nanotechnol. 6 (2011) 815–823.
[34] American Cancer Society, Cancer Facts & Figs. 2011, Epidemiologic Surveillance Report, American Cancer Society, Atlanta, 2011, (available at: <http://www.cancer.org/acs/groups/content/@epidemiologysurveilance/documents/document/acspc-029771.pdf>. Accessed April 2013).
[35] A. Jemal, R. Siegel, J. Xu, E. Ward, Cancer statistics, 2010, CA Cancer J. Clin. 260 (2010) 277–300.
[36] F. Pampaloni, E.G. Reynaud, E.H.K. Stelzer, The third dimension bridges the gap between cell culture and live tissue, Nat. Rev. Mol. Cell Biol. 8 (2007) 839–845.
[37] N.J. Yoo, S.Y. Hur, M.S. Kim, J.Y. Lee, S.H. Lee, Immunohistochemical analysis of RNA-induced silencing complex-related proteins AGO2 and TNRC6A in prostate and esophageal cancers, APMIS 118 (2010) 271–276.
[38] T. Endo, K. Itaka, M. Shioyama, S. Uchida, K. Kataoka, Gene transfection to spheroid culture system on micropatterned culture plate by polyplex nanomicelle: a novel platform of genetically-modified cell transplantation, Drug Deliv. Transl. Res. 2 (2012) 398–405.

Cyclic RGD-Linked Polymeric Micelles for Targeted Delivery of Platinum Anticancer Drugs to Glioblastoma through the Blood–Brain Tumor Barrier

Yutaka Miura,[†,‡,§] Tomoya Takenaka,[†] Kazuko Toh,[§] Shourong Wu,[§] Hiroshi Nishihara,[△] Mitsunobu R. Kano,[∥] Yasushi Ino,[⊥] Takahiro Nomoto,[#] Yu Matsumoto,[§] Hiroyuki Koyama,[‡] Horacio Cabral,[#] Nobuhiro Nishiyama,[○,*] and Kazunori Kataoka[†,◇,§,*]

[†]Department of Materials Engineering, Graduate School of Engineering, The University of Tokyo, 7-3-1 Hongo, Bunkyo-ku, Tokyo 113-8656, Japan, [‡]Division of Tissue Engineering, Graduate School of Medicine, The University of Tokyo, 7-3-1 Hongo, Bunkyo-ku, Tokyo 113-8655, Japan, [§]Center for Disease Biology and Integrative Medicine, Graduate School of Medicine, The University of Tokyo, 7-3-1 Hongo, Bunkyo-ku, Tokyo 113-0033, Japan, [△]Department of Translational Pathology, Graduate School of Medicine, Hokkaido University, N15W7, Kita-ku, Sapporo 060-8638, Japan, [∥]Department of Pharmaceutical Biomedicine, Graduate School of Medicine, Dentistry, and Pharmaceutical Science, Okayama University, 1-1-1 Tsushima-naka, Kita-ku, Okayama 700-8530, Japan, [⊥]Division of Innovative Cancer Therapy, The Institute of Medical Science, The University of Tokyo, 4-6-1 Shirokanedai, Minato-ku, Tokyo 108-8639, Japan, [#]Department of Bioengineering, Graduate School of Engineering, The University of Tokyo, 7-3-1 Hongo, Bunkyo-ku, Tokyo 113-8656, Japan, [○]Polymer Chemistry Division, Chemical Resources Laboratory, Tokyo Institute of Technology, R1-11, 4259 Nagatsuta, Midori-ku, Yokohama 226-8503, Japan, and [◇]Center for NanoBio Integration, The University of Tokyo, 7-3-1 Hongo, Bunkyo-ku, Tokyo 113-8656, Japan

ABSTRACT Ligand-mediated drug delivery systems have enormous potential for improving the efficacy of cancer treatment. In particular, Arg-Gly-Asp peptides are promising ligand molecules for targeting $\alpha_v\beta_3/\alpha_v\beta_5$ integrins, which are overexpressed in angiogenic sites and tumors, such as intractable human glioblastoma (U87MG). We here achieved highly efficient drug delivery to U87MG tumors by using a platinum anticancer drug-incorporating polymeric micelle (PM) with cyclic Arg-Gly-Asp (cRGD) ligand molecules. Intravital confocal laser scanning microscopy revealed that the cRGD-linked polymeric micelles (cRGD/m) accumulated rapidly and had high permeability from vessels into the tumor parenchyma compared with the PM having nontargeted ligand, "cyclic-Arg-Ala-Asp" (cRAD). As both cRGD/m- and cRAD-linked polymeric micelles have similar characteristics, including their size, surface charge, and the amount of incorporated drugs, it is likely that the selective and accelerated accumulation of cRGD/m into tumors occurred *via* an active internalization pathway, possibly transcytosis, thereby producing significant antitumor effects in an orthotopic mouse model of U87MG human glioblastoma.

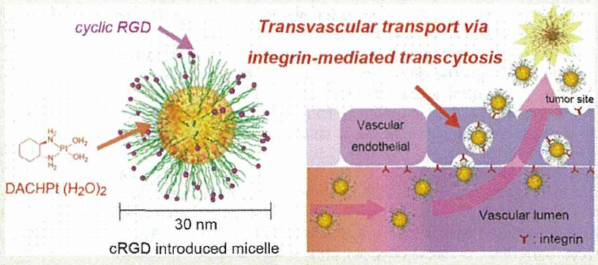

KEYWORDS: drug delivery · block copolymer · polymeric micelle · integrin · cRGD · cancer therapy

Treatment of glioblastoma (GBM) is one of the greatest challenges in cancer therapy.[1−4] Although a large number of advanced treatment paradigms have had impacts on medical management for other tumors, prolongation of GBM patients' survival has not been achieved in decades.[5−9] Because of the difficulty of complete surgical excision, irradiation and chemotherapy play important roles in conventional GBM treatment. However, the effects of chemotherapy on GBM are very limited as a result of poor drug penetration from vessels into tumors caused by the vascular/tumor barrier such as the blood–brain barrier (BBB) and the blood–brain tumor barrier (BBTB).[10−15] In fact, the vascular/tumor barrier is highly variable and heterogeneous in the brain. At the early stage of GBM, the tumor cells use the normal brain vessels, which are protected by the BBB, for their growth.[11,13−17] The gradual progression of GBM and its neovascularization compromise the integrity of BBB and lead to the formation of BBTB.[11,16,17] By the time GBM is diagnosed,

* Address correspondence to kataoka@bmw.t.u-tokyo.ac.jp; nishiyama@res.titech.ac.jp.

Received for review May 27, 2013 and accepted September 12, 2013.

Published online September 12, 2013
10.1021/nn402662d